

# OFDM-Based Common Control Channel Design for Cognitive Radio Ad Hoc Networks

Kaushik R. Chowdhury, *Member, IEEE*, and Ian F. Akyildiz, *Fellow, IEEE*

**Abstract**—Cognitive radio (CR) technology allows devices to opportunistically use the vacant portions of the licensed wireless spectrum. However, the available spectrum changes dynamically with the primary user (PU) activity, necessitating frequent PU sensing coordination and exchanging network topology information in a multihop CR ad hoc network. To facilitate these tasks, an always-on, out-of-band common control channel (CCC) design is proposed that uses noncontiguous OFDM subcarriers placed within the guard bands separating the channels of the licensed spectrum. First, the task of choosing the OFDM-specific parameters, including the number, power, and bandwidth of the subcarriers is formulated as a feasibility problem to ensure that the CCC does not adversely interfere with the PU operation. Second, for unicast messaging between a given pair of users, a subset of the guard bands may be chosen, which allows an additional measure of protection for the adjacent PU spectrum. For this, the multiarm bandit algorithm is used that allows the guard band selection to evolve over time based on the observed interference from the PU. Results reveal that our proposed CCC ensures connectivity and improved PU protection with a limited trade-off in data rate when compared to frequency-hopping and cluster-based CCC schemes.

**Index Terms**—Ad hoc networks, cognitive radio, control channel, feasibility.

## 1 INTRODUCTION

THE recent advancements in radio hardware and changes in the spectrum regulation policy of the Federal Communications Commission (FCC) have allowed the opportunistic use of portions of the licensed spectrum by unlicensed users. Cognitive radio (CR) is envisaged as the key enabling technology that allows the CR users to detect the spectrum availability, share the spectrum resource, and adapt to changes in its availability, so that the licensed or primary users (PUs) are unaffected [1]. Specifically, in CR ad hoc networks, nodes must undertake these spectrum-related functions in the absence of a central controller, and also maintain end-to-end coordination spanning multiple hops. In such cases, the coordination must occur over a common control channel (CCC) that is not interrupted by the changing PU activity, thereby ensuring a continuously available connection between the CR devices.

The need for a CCC is evident in the four main functions of a CR network, namely, spectrum sensing, sharing, decision, and mobility [1], each of which involves extensive control messaging. In *spectrum sensing*, other CR users in the neighborhood of the sensing CR node must be informed to maintain silent periods, which improves the sensing accuracy. Moreover, the sensing results need to be disseminated to these neighbors. Game-theoretic methods are often used in *spectrum sharing*, where each CR

user is a player of the game and must compete for the available spectrum. The bids and strategies of one player must be conveyed to the other participants of the game over multiple iterations. In multihop networks, the choice of the path and the spectrum are jointly undertaken as part of the *spectrum decision* function. The route setup process generally involves a partial or network-wide broadcast messaging, and the final path is chosen based on the spectrum availability information collected at the destination. Similarly, when a spectrum is no longer available, the affected node pair must coordinate with each other to simultaneously switch to a new mutually acceptable channel as part of the *spectrum mobility* function. In all the above cases, the reliable delivery of the control messages is a key factor in ensuring the smooth operation of the protocols. As the transmission and reception of these control messages must not be impaired, we believe that the CCC must be *always-on*, even under the fluctuating spectrum availability.

In this paper, we propose the use of the guard bands between the channels of the licensed spectrum for an out-of-band CCC. The comparatively small portions of the frequency space contained in the guard bands serve as *buffers* between two adjacent PU channels. As an example, the television transmitters operate in three bands—low-band VHF for channels 2-6 (54-88 MHz), high-band VHF for channels 7-13 (174-216 MHz), and UHF for channels 14-83 (470-890 MHz). Such television towers may be considered as PUs, having channels that are generally 6 MHz wide, and guard bands ranging from 0.5 to 1 MHz. In our approach, a limited number of Orthogonal Frequency-Division Multiplexing (OFDM) subcarriers are inserted in each guard band. The CR users may decide in a distributed manner which of these subcarriers are *active* at a given time, and these active subcarriers, considered together, compose the CCC. Fig. 1 shows our proposed CCC design with the guard bands

• K.R. Chowdhury is with the Department of Electrical and Computer Engineering, Northeastern University, 308 Dana Research Center, 360 Huntington Ave, Boston, MA 02115. E-mail: krc@ece.neu.edu.

• I.F. Akyildiz is with the Broadband Wireless Networking Laboratory, School of Electrical and Computer Engineering, Georgia Institute of Technology, Centergy One, Room 5170, Atlanta, GA 30332. E-mail: ian@ece.gatech.edu.

Manuscript received 26 May 2009; revised 25 Nov. 2009; accepted 28 Feb. 2010; published online 26 Aug. 2010.

For information on obtaining reprints of this article, please send e-mail to: tmc@computer.org, and reference IEEECS Log Number TMC-2009-05-0192. Digital Object Identifier no. 10.1109/TMC.2010.160.

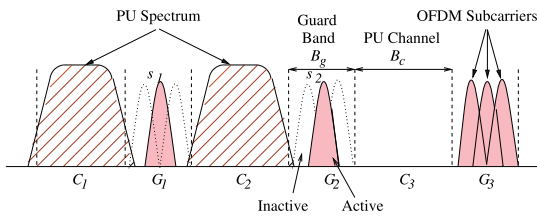


Fig. 1. CCC operation using guard bands in the licensed spectrum.

$G_1 - G_3$  between the PU channels  $C_1 - C_3$ , respectively. The guard bands of bandwidth  $B_g$  are smaller than the PU channels of bandwidth  $B_c$ , and have three OFDM subcarriers each. The *active* subcarriers are indicated as filled. In OFDM, the data stream from the sender is divided among several subcarriers. The more the number of subcarriers, the greater is the effective rate of the CCC. However, OFDM-specific transmission requirements, the bandwidth of the guard bands, and the interference of the subcarriers at the edge of the PU spectrum are some of the factors that limit the number and bandwidth of the subcarriers.

Our proposed CCC design is undertaken in two stages to meet the performance constraints of the CR and PU networks. In the first stage, the parameters of the subcarriers, such as the transmit power, bandwidth, and the maximum possible number in a guard band are decided based on the constraints of OFDM technology, and the permissible levels of spectral overlap with the PU transmission. This stage is modeled as a feasibility problem, which is solved before the CR network is in operation. As an example, Fig. 1 shows each guard band containing three OFDM subcarriers.

In the second stage, the CR nodes choose which of the guard bands (and hence, the subcarriers contained in them) should be activated, based on the local observed PU activity. The need for this adaptation is important as there may be a deviation from the specification in the PU spectrum caused by equipment aging, or a change in the established PU standards *after* the CR network is deployed. Moreover, certain PUs, such as television stations using Vestigial Sideband (VSB) modulation, may need stronger protection in the lower frequencies of the channel that contain the synchronization pilot. In Fig. 1, the subcarriers in the guard bands  $G_1$  and  $G_2$  are rendered *inactive* as they have a higher probability of interference with the PU spectrum in the licensed channels  $C_1$  and  $C_2$ , while there is no such constraint in the vacant channel  $C_3$ . The second phase of the CCC allows each CR user pair to independently adapt the subcarrier choices. This adaptation is achieved by using the Bandit Algorithm [2] that assigns a reward for a given selection of the guard band (and hence, the subcarriers) based on the effect of the PU transmission spectrum. The reward determines the probabilities with which a specific guard band combination is chosen in the next round of communication, and this choice gets progressively refined with time. Decisions based on merely current observations fail to capture the underlying characteristic of the channel, rely on accurate sensing, and do not proactively anticipate interference conditions.

Our CCC design supports both broadcast and pairwise unicast communication. Broadcasting is useful during route

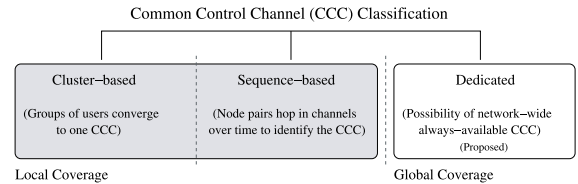


Fig. 2. Common control channel design classification.

formation or neighbor discovery, but it is a challenge to find a common channel suitable for all the neighbors. Broadcasting on all the licensed channels introduces a higher probability of interference to the PUs. Instead, our CCC activates only the central subcarriers of all the guard bands, thereby maximizing the protection to the PUs but incurring a trade-off by lowering the link data rate. For unicast communication, in addition to the central subcarriers, some of the other guard bands are rendered *active*, meaning that all the subcarriers contained in them are used. In Fig. 1, apart from the central subcarriers  $G_1$  and  $G_2$ , all the subcarriers in guard band  $G_3$  are active. As the specific guard bands used for the CCC are learned over time, the CR network can now maximize its link data rate (by using more subcarriers) and yet maintain an adequate level of frequency separation from the PU spectrum. Here, we note that each CR user perceives a different PU interference environment based on its location. Thus, the specific guard bands used for pairwise communication may be different for each individual CR user. We do not, however, propose a complete MAC protocol. Rather, we provide the design of the control channel that can be used by *any* legacy MAC providing channel access and error recovery mechanisms.

In summary, the contributions made in this paper toward the design of a CCC for CR networks are twofold:

- A novel approach of using guard bands for the CCC is proposed that ensures uninterrupted control messaging over the primary channel.
- The choice of the guard bands used for the CCC evolves over time, and our learning framework allows the CR users to adapt to the PU operation without prior statistical information.

The rest of this paper is organized as follows: Section 2 describes the related work in this area. This is followed by the feasibility framework for determining the OFDM-specific subcarrier parameters in Section 3. A detailed description of the operation of the CCC for broadcast and unicast transmissions is given in Section 4. A thorough performance evaluation is conducted in Section 5. Finally, Section 6 concludes our work.

## 2 RELATED WORK

As shown in Fig. 2, the current control channel design approaches can be classified into three functional groups: 1) cluster-based, 2) sequence-based, and 3) dedicated CCC, which we describe in detail in this section. Additionally, the control channel designs can be further categorized into *local* and *global* coverage, depending on the extent of the physical region that the CCC covers.

## 2.1 Cluster-Based CCC

Here, a number of CR users form *clusters*, and a common CCC is chosen for all of them. This grouping of nodes may be based on their physical proximity, spectrum usage conditions, and other common environmental factors. In [4], a swarm-intelligence-based algorithm is proposed that adaptively selects the CCC based on the preferences of the neighbor nodes. Each user chooses an initial *master* channel and transmits in it with higher probability, as compared to the remaining channels. An interference-based ranking of the channels is continuously transmitted by the CR users. A given user chooses that particular channel as the CCC that has the comparatively higher rank among its neighbors. This scheme of CCC determination uses several rounds of negotiation which are undertaken on the standard PU channels, which may interfere with the PU transmissions. Similarly, there is no guarantee that 1) nodes will converge to a single choice for the control channel, and 2) the system will not enter into oscillations. Similar cluster-based approaches are given in [3] and [20], where the size of the collaborating set of users, and location-dependent spectrum availability are considered for deciding the control channel. However, how these clusters are formed in a distributed manner *before* establishing the CCC is a primary concern.

## 2.2 Sequence-Based CCC

Here, the CR users tune themselves to the PU channels in a pseudorandom or predecided sequence, till they arrive at a common channel with the neighbors. In [11], the CR users broadcast their available channels in *all* the  $N_c$  licensed channels. This allows the neighboring users to update the list of channels they have in common with the sender. Moreover, time is divided into  $N_c$  slots, and each slot is assigned to one of the channels at the start. The CR user must wait for the slot corresponding to the channel it has in common with its neighbors before proceeding with the data transmission. Instead of a static channel slot allotment, the hopping sequence of the nodes can be pseudorandom, as seen in [7]. The CR users hop on a set of channels in a sequence that may differ from those of their neighbors, and continuously transmit packets when they need to establish a link. Once a node pair exchanges the synchronization packets on a common channel, called as the *rendezvous* channel, they may decide a common hopping sequence for the data transfer. However, the broadcasting of the available channels by the CR users in [7], [11] without considering the effect on the PUs limits severely their practicality. Second, there is a considerable synchronization time for which no useful communication occurs, and the opportunity for using the spectrum is lost.

# 3 CCC SUBCARRIER ALLOCATION

## 3.1 Dedicated CCC

Several recent works in MAC protocols for CR networks [6] assume the presence of a dedicated CCC that is assigned to all the users [5], [9], [10], [12], [18]. Though these works do not specifically describe the design of such control channel, there is a clear motivation to provide an always available and networkwide CCC that could be used for broadcast messaging, in addition to pairwise communication between

the CR users. Such an always available CCC is more efficient in spectrum utilization, as opposed to the *sequence-based* design, which needs a prolonged synchronization time during the channel hopping. Moreover, unlike *cluster-based* approaches, a network-wide CCC has lower coordination overhead between groups of CR users. This also allows for scalability, and does not need maintaining specialized network topologies for the CCC operation.

The channel for the dedicated CCC must be carefully chosen, so that it is not interrupted over long periods of time. While this considerably simplifies the CCC operation, the main difficulty is identifying a uniformly acceptable channel throughout the entire network. Moreover, care should be taken to ensure that the CCC does not lower the spectrum utilization efficiency in low-traffic scenarios, as spectrum for the control messaging is exclusively reserved. Our proposed OFDM-based CCC design using guard bands addresses these concerns so that the CR users have a reliable channel for exchanging critical spectrum information, even during dynamically varying spectrum activity. Moreover, it improves the spectrum utilization, and allows fast recovery for the link spectrum during sudden PU appearance, as we describe in Section 3.2.

Our proposed CCC design is composed of two stages, called as the 1) OFDM subcarrier allocation stage, and the 2) CCC operation stage, respectively. The first stage of deciding the OFDM-specific subcarrier parameters is done before the network initialization, and is described in this section. Specifically, a feasibility framework is devised that allows the selection of the OFDM subcarrier bandwidth, the maximum number of subcarriers per guard band, symbol preamble time, and the transmit power. However, not all the allowed subcarriers may be active at the same time. The choice of the active guard bands (and hence, the subcarriers) is done in the second stage, once the CR network begins operation, which is described later in Section 4.

## 3.2 OFDM-Based Feasibility Framework for Subcarrier Allocation

In this stage, the OFDM subcarrier parameters are designed based on the channel structure of the licensed spectrum. This design process is composed of the following two steps:

1. The entire licensed spectrum is considered as a contiguous set of OFDM subcarriers. First, all the subcarriers overlapping with the primary channels are rendered inactive, as they cannot be used in our *always-on* CCC. As an example, the subcarriers that overlap with channels  $C_1$ ,  $C_2$ , and  $C_3$  in Fig. 1, are made inactive.
2. For the remaining subcarriers in the different guard bands ( $G_1$ ,  $G_2$ , and  $G_3$  in Fig. 1), we formulate a feasibility problem that aims to find the subcarrier bandwidth (hence, their number), OFDM preamble time, and transmit power, so that
  - a. the PU network is protected,
  - b. the CR CCC data rate is maximized,
  - c. the network connectivity is maintained, and
  - d. hardware or OFDM-specific constraints are met.

TABLE 1  
Symbols Used in the Feasibility Framework

Symbol	Description
$n$	Number of CR users
$s_{a_n}(t)$	Time domain signal for the $a_n$ <sup>th</sup> subcarrier
$d(a_n)$	Data rate for the $a_n$ <sup>th</sup> subcarrier
$D_{min}$	Minimum required data rate
$N_g$	Number of guard bands in the licensed spectrum
$m$	Number of OFDM subcarriers in a guard band
$\tau$	Time for transmitting one OFDM symbol
$t_g$	Guard time between two OFDM symbols
$\alpha, \beta$	Free space propagation constants
$P_{tx}$	CR OFDM subcarrier transmission power
$P_R^T$	CR receiver threshold power
$R_{min}$	Minimum CR transmission range
$v$	Node velocity
$p$	Pause time between successive displacements
$B_g$	Guard band bandwidth
$B_c$	Licensed spectrum channel bandwidth
$B_s$	Bandwidth of a single OFDM subcarrier
$O_t$	Interference power overlap threshold for PUs

Next, we describe our framework using the symbols summarized in Table 1.

Given :  $B_c, B_g, N_g, D_{min}, P_{max}, R_{min}, PAPR_{max}, t_g$   
 To find :  $m, \tau, P_{tx}$  (1)  
 Subject to :

$$\int_0^\tau s_{a_1}(t) \cdot s_{a_2}(t) dt = \begin{cases} 0, & a_1 \neq a_2 \\ \frac{\tau}{2}, & a_1 = a_2 \end{cases} \quad (2)$$

where

$$s_{a_n}(t) = \cos\left(\frac{2\pi a_n}{\tau} \cdot t + \theta_{a_n}\right) a_n \in [1, m \cdot N_g] \quad (3)$$

$$\frac{1}{\tau} \cdot (1 + m) \leq B_g \quad (4)$$

$$m \cdot N_g \leq PAPR_{max} \quad (5)$$

$$\left[\frac{P_{tx} \cdot \alpha}{P_R^T}\right]^\frac{1}{\beta} \geq R_{min} \quad (6)$$

$$\sum_{i=1}^{N_g} d(i) \geq D_{min}, \quad (7)$$

$$t_g + \tau < T_{min} \quad (8)$$

In this framework, we are given the primary channel bandwidth ( $B_c$ ), the number of guard bands ( $N_g$ ) and their associated bandwidth  $B_g$  in the licensed spectrum, apart from the OFDM-specific transmission thresholds. In (1), our framework attempts to find the number of OFDM subcarriers

( $m$ ), the time for a single symbol pulse ( $\tau$ ), and the transmit power ( $P_{tx}$ ) for the pulses. The constraints which govern the functioning are:

- The principle of orthogonality of the OFDM subcarriers is captured in (2). Here, each subcarrier must be separated by an integral multiple of the bandwidth  $\frac{1}{\tau}$  in the frequency domain.
- The choice of the number of subcarriers should be such that when placed contiguously in the frequency domain, their collective bandwidth must be contained within the guard band boundaries, as shown in (3).
- A high OFDM peak to average power ratio (PAPR) may affect the signal quality, as the nonlinear components of the transceiver circuits may distort the modulation and the signal constellation. Unlike the classical OFDM that assumes the symbols to be identically and independently distributed, a large number of subcarriers (overlapping with the PU channels) are *always* inactive in our proposed CCC design. Thus, in (4), we consider the limiting PAPR for the NC-OFDM system,  $PAPR_{max} \geq m \cdot N_g$ , where  $m \cdot N_g$  is the maximum possible number of active subcarriers [16].
- While the transmit power  $P_{tx}$  of the CR users must satisfy the PAPR limit, it must also be sufficient to maintain connectivity in the network, as given in constraint (5). The minimum transmission range for a mobile network exhibiting random waypoint mobility is given by  $R_{min} = \frac{p+0.521405}{p} \sqrt{\frac{\ln n}{\pi n}}$ , where  $n$ ,  $p > 0$  and  $v > 0$  are the number of users, pause time, and node velocity, respectively [19]. The transmit power is chosen such that for a simple path loss propagation model, and a given receiver sensitivity threshold  $P_R^T$ , the range is at least  $R_{min} \cdot \alpha$  and  $\beta$  are the free space path loss constants.
- The minimum number of active subcarriers ( $N_g$ ) are the central subcarriers of all the guard bands, which we describe in detail in Section 4.1. The data rate provided in this case must be sufficient to meet the minimum expected rate  $D_{min}$ , shown in (6).
- The inverse relationship between the time-domain OFDM symbol time and the frequency-domain subcarrier bandwidth necessitates limiting the time required for transmitting the OFDM symbol, as given in (7). A larger symbol time  $\tau$  results in shorter subcarrier bandwidth, thereby allowing more subcarriers to be accommodated with a guard band. However, for fair channel access, the transmission of a symbol for each CR user must be completed within a limit  $T_{min}^s$ . Moreover, the additional cyclic prefix time  $t_g$  included at the start of each symbol to combat intersymbol interference (ISI) arising from multipath effects must also be considered. The 802.11a specification lists  $t_g = 800$  ns for a symbol time of  $\tau = 4$   $\mu$ s.
- Finally, (8) limits the cumulative effect of the subcarrier spectrum on the edge of the guard band. As shown in Fig. 3, the *sinc* function has harmonics

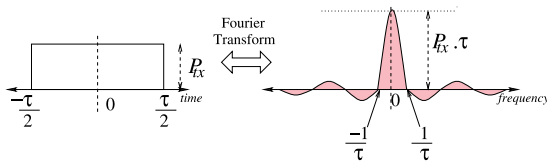


Fig. 3. The relationship between the transmission symbol and its frequency-domain sinc function.

with decreasing amplitude at intervals of  $\frac{1}{\tau}$ . For a given subcarrier, we integrate the power contributed by the harmonics over the range of the PU channel bandwidth to estimate the interference caused by it. For this, we begin with the central subcarrier (at a distance of  $\frac{B_g}{2}$  from the edge of the guard band) and consider the frequency at the other end of the PU channel ( $\frac{B_g}{2} + B_c$ ), thereby giving the limits of integration. The effect of the other  $\frac{m-1}{2}$  subcarriers placed between the center to the end of the guard band is similarly considered, thereby giving the limits of the outer summation. Finally, from symmetrical considerations of guard bands being placed on either end of the PU spectrum, this interference is scaled by 2. Here, the value  $O_t$  is a predetermined hard threshold on the transmit power for each CR transmitter. We reason that the PU, in the worst case, could be colocated with the CR transmitter. Hence, each CR user must set an upper limit on its own overlapping power induced by harmonics.

The results of this feasibility analysis define the CCC structure used by the CR users. In the event that a spectrum band does not satisfy these constraints, we do not allow its use by the CR for the CCC. In the unlikely case that no feasible spectrum band exists, the CR users fall back to the ISM band for the CCC, thereby incurring a higher switching latency (hence, lower throughput) as it alternates between the licensed and the ISM spectrum bands for data and control messages, respectively.

In Section 4, we describe how the CR users choose the active subcarriers by adapting the CCC operation based on their perceived local PU activity and the function in the network.

## 4 CCC OPERATION

In Section 3.2, we described the procedure for choosing the OFDM subcarrier parameters for use as the CCC. In this section, we demonstrate how specific CCC operations, such as 1) broadcast, and 2) unicast messaging are facilitated by our design. In each case, a different set of subcarriers is rendered *active*, so that possible interference-related adverse effects on the PU performance are minimized.

### 4.1 Broadcast Messaging

Broadcasting is important for the operation of higher layer protocols, in which more than one CR user may be the recipient of the message. Typical examples would be *hello* packet exchange during neighbor discovery, RTS-CTS handshake at the link layer, route request packets sent at the network layer, among others. A CR user may not have knowledge of the presence of the PUs in a region outside its

immediate sensing range. As a result, broadcast messages, say in the case of neighbor discovery, sent by the CR user on the licensed channels may interfere with ongoing PU transmissions. Our proposed scheme addresses these concerns by only rendering the central subcarriers active in each guard band. We describe our method in detail as follows:

Consider a broadcast packet transmitted by a CR user using the set of central subcarriers in each guard band. The central subcarrier of a guard band has the largest frequency separation between itself and the PU spectrum in its adjacent licensed channels. Hence, the new CR user may use this set of central subcarriers ( $\eta$ ) for maximum protection to the PU network during the broadcast, when it is unaware of the spectrum usage in its neighborhood. The trade-off in this method is that the use of only one subcarrier per guard band lowers the data rate, resulting in the channel being captured for a comparatively longer time for the broadcast.

Here, the data rate  $D_B$  of the broadcast packet must be at least equal to  $D_{min}$ , as defined in Section 3.2. Formally,  $D_B$  is the cumulative sum of the individual data rates  $d(k_i)$  of the *active* subcarriers  $k_i$ ,  $i = 1, \dots, N_g$  given by

$$D_B = \sum_{i=1}^{N_g} d(i) \quad (9)$$

$$= N_g \cdot \frac{\psi}{t_g + \tau}. \quad (10)$$

The data rate  $d(i)$  of a subcarrier  $i$  can be expressed as the ratio of  $\psi$  (the number of bits per OFDM symbol) to the time taken for transmitting one symbol ( $\tau$ ) and the guard time ( $t_g$ ) inserted to combat the ISI. In our case, we assume BPSK modulation that gives  $\psi = 1$  bits/symbol.

The center frequencies  $F_i$  of the set of the central OFDM subcarriers  $i \in \eta$  are given by the following theorem:

**Theorem 1.** Let  $i = 1, \dots, N_g$  represent the ID of the central OFDM subcarriers of the  $N_g$  guard bands, each having a subcarrier bandwidth of  $B_s$ . If the bandwidth of the PU channels and the guard bands separating them are  $B_c$  and  $B_g$ , respectively, then

$$F_i = \begin{cases} \frac{2B_c + B_g}{B_s}, & i = 1, \\ 2 \cdot F_{i-1} + \frac{B_g}{B_s}, & 1 < i \leq N_g. \end{cases} \quad (11)$$

**Proof.** Proof is included in the Appendix.  $\square$

Thus, by activating the above set of subcarriers, the new CR user ensures that its broadcast message is heard by the other existing users in the network with minimum effect on the PU network. In the possible event that one of the central subcarriers of a user  $x$  is not correctly tuned due to equipment malfunction, the broadcast mechanism is slightly altered. All the neighbors of  $x$  must now undertake a two-stage broadcast, in which, the first stage proceeds along the lines described above. In the second stage, the broadcast is repeated with the central subcarriers that  $x$  currently supports. However, hardware faults, being more of an exception, do not impair the general performance of our proposed CCC.

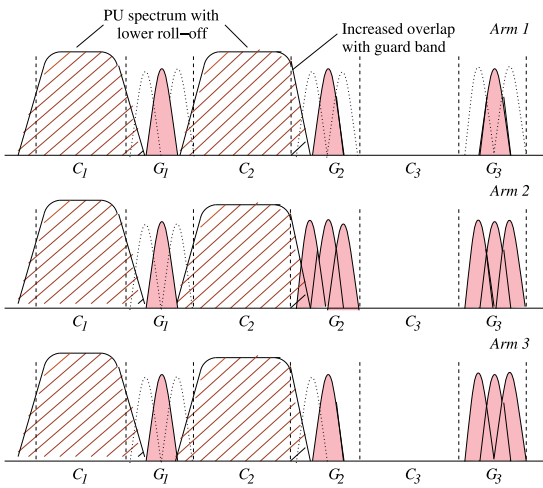


Fig. 4. The arms formed by the choice of guard bands.

## 4.2 Unicast Messaging

Once the CR users are part of the network, they periodically exchange unicast packets with their neighboring nodes. This exchange may be concerned with exchanging synchronization packets, coordinating the choice of the licensed spectrum and channel before beginning the actual data transfer, among others. In Section 3.2, the framework derived the maximum number and bandwidth of the subcarriers. However, during the operation of the CR network, there may be certain practical conditions listed below that are not considered at the time of node deployment. Thus, the CR users continue to refine their choices of the active guard bands and learn of the best combination of the guard band over time. The learning process allows a proactive interference avoidance by estimating in advance which is the best choice of guard bands based on the past experience of the node.

- *PU Spectrum Distortion*: The fall in the PU spectrum curve (Fig. 4) at the edge of the channel boundary is determined by the bandpass filter rolloff factor. Due to equipment aging or malfunction, the actual rolloff may deviate from the specifications. This may result in greater overlap of between the PU and CR spectra, leading to increased interference.
- *Specific Transmission Technologies*: The information contained in the PU spectrum may not be uniformly distributed over the entire channel bandwidth. As an example, in the digital television systems using vestigial sideband modulation (VSB), a pilot signal is inserted about 0.31 MHz from the lower edge of the channel, which enables receiver tuning under noisy conditions. Thus, one edge of the PU spectrum may be more susceptible to interference, and simply bounding the overlap between the spectra may not capture the true interference to the PU.
- *Effect of Frequency Harmonics*: The OFDM subcarrier spectrum, represented by the *sinc* function in Fig. 3, extends beyond the  $|\frac{1}{\tau}|$  interval on either side of the frequency axis. Some guard band intervals may particularly experience a high level of destructive combination of these harmonics, and hence, must be avoided.

### 4.2.1 Bandit Algorithm Preliminaries

Our proposed CCC scheme allows each CR user to learn which guard bands are affected by the above, by observing the signal strength at the receiver side. We use the multiarm bandit algorithm, in which, each arm is analogous to a *slot machine* that returns a specific reward on being played [2]. There are several possible arms and the user has no prior knowledge of the arms that yield higher rewards. The user may continue to *exploit* the current choice of the arm, and get the known level of reward, or choose to *explore* a new arm. For a new arm, the users run the risk of lowering the reward, thus incurring an adverse cost for the exploration. At the same time, it may be possible that the reward associated with the new arm is significantly higher, making it worthwhile to conduct the exploration. The main advantage of using the bandit algorithm is that it tries to balance the cost of exploitation and exploration, so that the cumulative reward of the user ( $R_c$ ) is within a bound of the maximum possible reward ( $R_{max}$ ). The difference between the observed and optimal values of the reward is called as the *regret* ( $R_R$ ). Hence,  $R_R = R_{max} - R_c$ , which is mathematically bounded in the limiting case of infinite trials by suitably altering the probability of choosing the arms after the current trial round.

### 4.2.2 Bandit Algorithm Application

In our approach, each feasible selection of the guard bands can be considered as an *arm*, as shown in Fig. 4. The rules for creating the arms are formally described as follows:

- A guard band is called as *active* (denoted by the integer 1, 0 otherwise) if all the subcarriers contained in it are used. Thus, the guard bands  $G_2$  and  $G_3$  used for the CCC (Arm 2 in Fig. 4) are *active*, while the guard band  $G_1$  is not.
- Irrespective of choice of the active guard bands, the central subcarriers are always used in all the  $N_g$  guard bands (e.g., Arm 1, where all the guard bands are inactive).
- An *arm* is a combination of guard bands, such as

$$\{\text{Arm1} : G_1 = 0, G_2 = 0, G_3 = 0\}, \{\text{Arm2} : G_1 = 0, G_2 = 1, G_3 = 1\},$$

and does not represent a guard band considered in isolation. If the number of guard bands  $N_g = 3$ , the number of possible arms ( $K$ ) is given by  $K = 2^{N_g} = 8$ .

In our example, the PUs on channels  $C_1$  and  $C_2$  have a wide spectrum shape caused by a lower rolloff factor, which is unknown to the CR network. During data transfer, the CR user at the receiver end measures the power individually in each guard band. By comparing this power against a predecided threshold, it determines the guard bands in which the PU spectrum overlap is excessive. In these guard bands, if certain subcarriers are lost (due to noise and destructive interference), or experience a reception power that is considerably higher (additive effect of the PU power spectrum or due to the harmonics of the other subcarriers), a negative reward is assigned to the arm. Similarly, the positive reward is given, if indeed the received power is contained within the allowed interference overlap threshold  $O_t$ . These rewards are cumulative, and

alter the probabilities with which the arm for the next packet transfer is chosen.

The transmitting CR user is allocated a reward for each choice of the arm by the receiver at the other end of the link. Similarly, other receiving neighbors, during subsequent communication, continue to modify the arm selection probabilities over time. Thus, when the algorithm converges to the final choice of the arm with the highest selection probability, it implies that the best selection of the guard bands is achieved for the given CR user (arm 3 in Fig. 4) considering the PU activity of all the receiving neighbors that it has communicated with over time.

The steps used to alter the arm selection probabilities for a given pair of CR users are described next, along the lines of the nonstochastic bandit algorithm [2].

#### Algorithm 1. Choosing the Arm

- 1: Initialization:  $w_i(t) = 1$  for  $i = 1, \dots, K$
- 2: Probability of choosing each arm:
- 3:  $p_i(t) = (1 - \gamma) \cdot \frac{w_i(t)}{\sum_{j=1}^K w_j(t)} + \frac{\gamma}{K}$
- 4: Send( $PKT_q^{s,r}$ ), where  $m \in [1, K]$

**Step 1—Choosing the arm.** At the initial time  $t = 0$ , the transmitting user ( $s$ ) initializes the arm weights  $w_i(t)$  to 1 for all the  $i = 1, \dots, K$  choices of the arms (Algorithm 1). It then picks one such arm  $q$  to form the CCC based on their respective selection probabilities  $p_i(t)$ . The algorithm uses two tuning parameters, given by  $\alpha = \frac{1}{T}$  and

$$\gamma = \min \left\{ 1, \sqrt{\frac{K(S \ln(KT)) + e}{(e-1)T}} \right\},$$

where  $T$  is the number of rounds of the arm selection [2].  $S$  is an upper limit of the *hardness* ( $H(j^T)$ ) of the sequence of actions ( $j_1, \dots, j_T$ ), and assumes the value  $T$  in the worst case (Section 4.2.3).

These parameters help to decide the arm selection probabilities as a function of their weight while keeping the regret  $R_R$  bounded (Section 4.2.3). Finally, the packet ( $PKT_q^{s,r}$ ) is sent by the CR user  $s$  to the intended receiver  $r$ , on the CCC by the selection of the  $q$ th arm. The bounded regret gives a limit on the performance loss of our approach, i.e., the extent of the interference-free transmission that is lost when the different arms are probabilistically explored.

**Step 2—Assigning the reward.** The receiver  $r$  receives the packet  $PKT_q^{s,r}$ , and identifies the set of subcarriers  $I$  that are either lost due to noise, or experience a signal power greater than the interference threshold  $P_I^T$  in all the guard bands used in the transmission. The receiver infers that these subcarriers experience a cumulative power gain caused by the spectrum leakage power from the PU transmissions. The reward  $R_c^q \in [0, 1]$  assigned by the receiver for the choice of this arm is given by

$$R_c^q = \left[ 1 - \frac{|I|}{m \cdot \nu} \right] \cdot \frac{m \cdot \nu + (N_g - \nu)}{m \cdot N_g}. \quad (12)$$

Here,  $\nu$  represents the number of guard bands used for the  $q$ th arm,  $m$  is the number of carriers in a guard band, and  $N_g$  is the number of guard bands. The first term of

the product term signifies the fractional number of interference-free subcarriers. The second term gives the ratio of the current data rate to the maximum possible data rate. There are also  $N_g - \nu$  central subcarriers that are active in the other unused guard bands that do not compose the arm.

The receiver  $r$  uses the central subcarriers of the guard bands (Section 4.1) for sending the ACK packet back to the sender  $s$  with the reward  $R_c^q$  for the  $q$ th arm piggybacked in this packet.

#### Algorithm 2. Update Arm Selection Probability

- 1: Update the weights of the arms:
- 2: **if**  $j == q, j \in [1, K]$  **then**
- 3:  $\hat{R}_c^j(t) = \frac{R_c^j(t)}{p_j(t)}$
- 4: **else**
- 5:  $\hat{R}_c^j(t) = 0$
- 6: **end if**
- 7:  $w_j(t+1) = w_j(t) \exp\left(\frac{\gamma \hat{R}_c^j(t)}{K}\right) + \frac{e\alpha}{K} \sum_{\rho=1}^K w_\rho(t)$

#### Step 3—Updating the arm selection probability.

Based on the reward earned on the choice of the arm, the weights  $w_j(t)$  influencing the probabilities of choosing the various arms are changed, as shown in Algorithm 2. For the active arm  $j = q$ , the earned reward  $R_c^j(t)$  is scaled by the probability of selection  $p_j(t)$ , and there is no update otherwise.

For the next packet sent by the CR user  $s$ , the new weights are used in order to calculate the probabilities of choosing the various arms  $p_i(t)$ , from Algorithm 1. Thus, for a given CR user, the choice of guard bands (hence, subcarriers) is refined to ensure that the specific interference environment is considered, and this occurs in a distributed manner during the normal operation of the network.

#### 4.2.3 Complexity and Bounds

The hardness of a sequence of actions ( $j_1, \dots, j_T$ ) is defined by  $H(j_1, \dots, j_T) = 1 + |\{1 \leq l < T : j_l \neq j_{l+1}\}|$  [2]. Thus, as  $S$  is the upper bound,  $H(j^T) \leq S$ . In the worst case, no arm  $j$  is chosen two consecutive times. This implies that  $\max\{S\} = T$ , and by choosing the tuning parameters  $\alpha$  and  $\gamma$ , as described above, the regret  $R_R$  follows the bound [2]:

$$R_R \leq 2\sqrt{(e-1)\gamma} \sqrt{SKT \ln(KT) + e}. \quad (13)$$

For the worst case, we substitute  $S = T$  in the complexity analysis of the regret, i.e.,  $O(T\sqrt{K \ln(KT)})$ . Interestingly, this bound holds for any finite  $T$ , and the stepwise regret can be calculated instead of considering only the limiting case of  $T \rightarrow \infty$ .

## 5 PERFORMANCE EVALUATION

In this section, we present simulation results to demonstrate the performance of the CR 1) *broadcast messaging* based on our subcarrier allocation (Section 4.1), and 2) *unicast messaging* supported by the bandit-algorithm-based learning (Section 4.2).

In our study, we used a custom-designed C++-based packet-level simulator that has a close coupling between the link and the physical layers, allowing easy sharing of

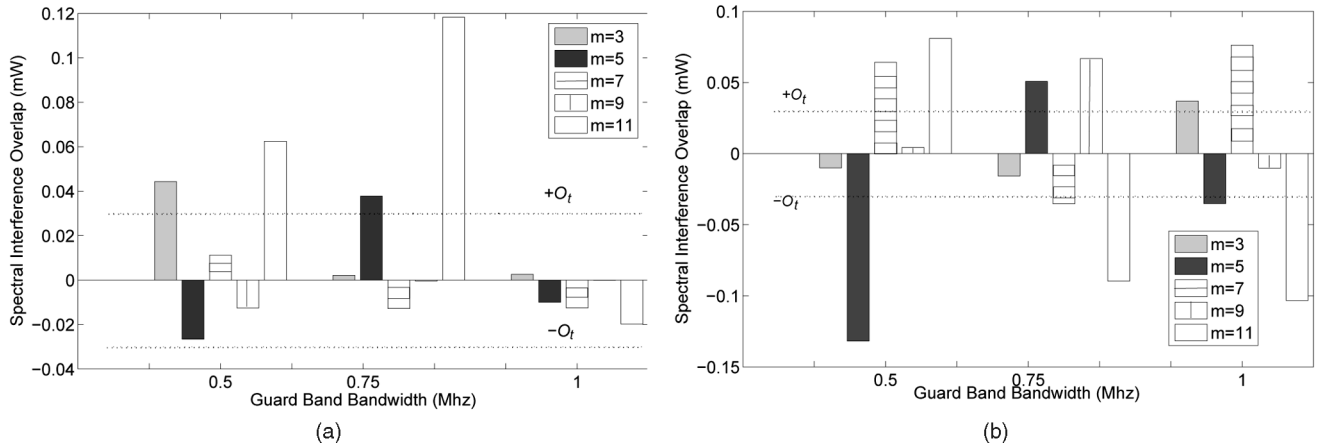


Fig. 5. The spectral interference overlap for (a) 6 and (b) 12 MHz licensed channels are shown, respectively.

information between them. The feasibility problem presented in Section 3.2 was implemented in MATLAB. We consider 10 licensed channels, with each channel being separated by a 0.75 MHz guard band, unless specified otherwise. The duration for which the channel is available, and the busy time resulting from the PU activity are exponentially distributed with means 10 and 20, respectively. The number of CR users varies from 25 to 150, and they are contained in a square region of side 1,000 m. The CR users move with a velocity of 1 m/s along a randomly chosen direction, and incur a pause time of 50s between two consecutive displacements. We use a CSMA/CA MAC layer based on the IEEE802.11b and assume a saturated network condition, where each user always has a 512 byte packet to transmit. The transmit range of the PU is 80 m and 20 stationary PUs are placed randomly in the area of study.

## 5.1 Broadcast Messaging

In the subsequent discussion, we shall use the following terminology for the schemes used in the comparative study:

- *O-CCC*: This is our proposed OFDM-based CCC scheme. Here, the guard time  $t_g$  is considered as  $\frac{1}{10}$  of the symbol time. The allowed PAPR threshold is set to 110 unless specified otherwise, and the receiver threshold is  $-85$  dBm.
- *Sequence*: A multiple-frequency hopping scheme is considered with a stay time of 0.5 s in each channel along the lines of the scheme proposed in [7]. Here, each CR user periodically transmits *hello* messages over pseudorandom hopping sequences till it synchronizes with its intended next hop neighbor.
- *Cluster*: This represents the swarm-based CCC formation scheme with similar parameters as used in [4]. The noise floor is set to  $-100$  dBm and the SNR ratio is calculated for each node by considering the total cumulative effect from all PUs.

Though our *O-CCC* scheme for broadcast (Section 4.1) minimizes the interference caused to the adjacent PU channels, the *sinc* function has harmonics that extend beyond the guard band. We measure the interference caused to a single PU by a given CR user considering the

licensed channel bandwidths of  $B_c = 6$  and  $B_c = 12$  MHz, in Figs. 5a and 5b, respectively. The number of subcarriers is varied each time from  $m = 3, \dots, 11$ , and their cumulative effect on the entire PU channel is noted. However, our framework limits the allowed choices of  $m$ . As an example, for the overlap threshold  $|O_t| = 0.03$  mW,  $B_c = 12$  MHz, and guard band of 0.75 MHz (Fig. 5b), our approach returns a usable transmit power of 1 mW (we consider discrete allowed power values only in the range  $[1, 0.001]$  mW in steps of 0.1), with  $m = 3$  subcarriers per guard band, each subcarrier being of bandwidth 160 KHz. Interestingly, the same number of subcarriers, i.e.,  $m = 3$ , is not suitable for a different PU channel bandwidth of  $B_c = 6$  MHz, as the threshold  $O_t$  is exceeded (Fig. 5a). Keeping the PU bandwidth constant, we observe that some choices of  $m$  may be acceptable for all choices of the guard band (such as  $m = 7$  in Fig. 5a). Similarly, some other choices of  $m$  may be unsuitable for all the guard band choices (such as  $m = 11$  in Fig. 5b). This nontrivial behavior results from the way in which the additive or subtractive components of the *sinc* functions are combined within the PU channel boundaries.

We next extend our simulation study to include the effect of multiple users in the network. First, we define a metric  $\Omega$  as the product of the interference caused to the PUs and the time for which this interference is in effect. The average value of  $\Omega$  per PU is shown in Fig. 6a for 100 random scenarios. Interestingly, this  $\Omega$  is prohibitively high for the *Cluster* method, for low number of CR users. Further investigation revealed that the swarm-based technique, in many topologies, forced a CR user to choose a channel that was occupied by a PU within its range. Though such CR users could successfully detect the presence of the PU, several of its neighbors were out of range of the PU. The cumulative preference of the neighbors outweighed the choice of the CR user, leading to higher local interference. For large number of CR users, more of the latter were under the PU coverage range at a given time, resulting in fewer cases of incorrect neighbor influence. Conversely, the *Sequence* scheme displays higher values of  $\Omega$  with increasing CR users. This is because there is a continuous broadcast on the channel, without special consideration to the presence of the PUs during the time used for synchronization. For

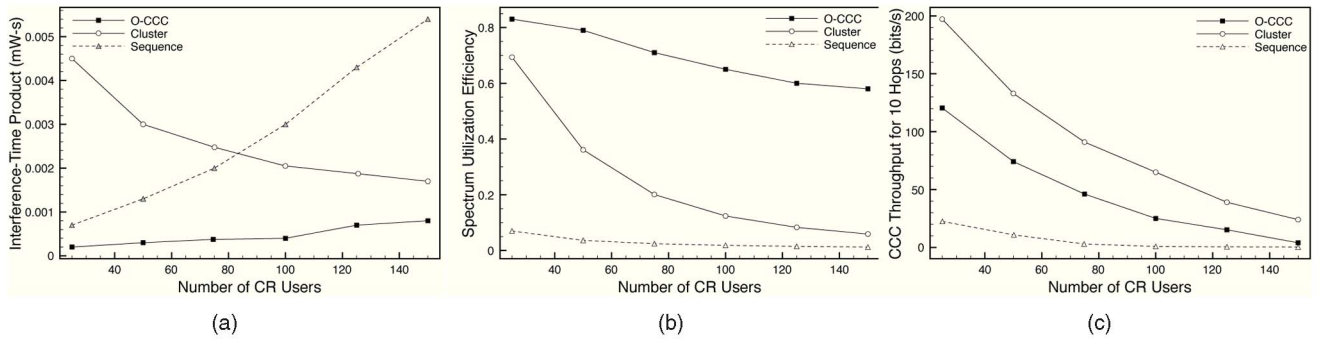


Fig. 6. The interference caused to (a) the PUs, (b) the spectrum utilization efficiency, and (c) throughput during CCC broadcast are shown, respectively.

large number of neighbors, each user must successively synchronize with all of them in turn, with a finite interference probability in each of the PU channels it tunes to during hopping. Our proposed *O-CCC* scheme introduced very limited interference owing to the use of the central subcarrier, and has a gradual rise in  $\Omega$  with the number of users.

The spectrum utilization efficiency measures the ratio of the time spent in useful transmission to the total time needed (averaged over all the CR users), inclusive of the time for establishing the connection (Fig. 6b). As *O-CCC* uses the *always available* guard band for the control broadcast, the connection establishment time is zero, thereby ideally giving an efficiency of 1. However, we notice a gradual decrease with the number of users, as each transmission also has a guard time per OFDM symbol to reduce the multipath effect. In comparison, the *Sequence* scheme has the lowest utilization as the channels are hopped in discrete intervals. Even after a user completes its broadcast, the next channel is switched only after its hopping duration on that channel is completed, thus reducing the utilization. The spectrum utilization in the *Cluster* scheme falls rapidly with increasing number of users as there are several rounds of message exchange between the CR users before a common CCC is determined.

The average CCC broadcast throughput is given for the scenarios in which the message is forwarded over 10 hops in Fig. 6c. Here, the *O-CCC* performs lower than the *Cluster* scheme. For the cluster scheme, we start the time counter *after* the control channel is determined. The effect on the *O-CCC* performance is seen because only a limited number of central subcarriers exist, lowering the effective link bandwidth and consequently, the end-to-end data rate. The long synchronization time of the *Sequence* scheme at each hop lowers the throughput significantly over multiple hops. The general fall in the *O-CCC* and *Cluster* curves for increasing number of CR users is attributed to the contention at the link, and has a similar effect on both these schemes.

## 5.2 Unicast Messaging

In this section, we evaluate how the gradual refinement of the subcarrier choices (Section 4.2) affects the network performance. Here, we decrease the rolloff factor of the PU curves from 0.5 to 0.2, leading to a greater overlap of the

PU spectrum with the guard band. This represents the cases in which the PU operational conditions change, possibly due to equipment malfunction, and this is unknown to the CR network.

In Fig. 7, we consider the *O-CCC* scheme with only the central subcarriers active, the proposed CCC scheme with the active subcarriers in the guard bands decided by the bandit algorithm (called as *CCC-Bandit*), and the case in which all the  $m \cdot N_g$  subcarriers are active (called as *CCC-All*). We observe that the interference contribution of the *CCC-Bandit* scheme is bounded between the two, when plotted against an increasing number of occupied PU channels. Moreover, the percentage increase in the interference is low in the *CCC-Bandit* scheme, as it manages to dynamically converge on the best set of guard bands (and hence, subcarriers), for a given PU occupancy.

In order to verify the fairness in the arm selection of our bandit-algorithm-based CCC, we define the metric *spectrum opportunity* or  $\Gamma$  that represents the number of trials undertaken for each arm. For two different cases of the number of occupied PU channels, Figs. 8a and 8b, the  $\Gamma$  is measured for each of the allowed arms on the x-axis. We observe that most of the arms lie in the range of  $\frac{1}{3}$ – $\frac{2}{3}$  of the maximum possible  $\Gamma$ . Thus, the arms are fairly explored, and the outliers (below  $\frac{1}{3}$  of the maximum  $\Gamma$ ) are very limited. Moreover, even when a large number of licensed channels are busy, say eight, as seen in Fig. 8b, the  $\Gamma$  does not vary significantly from the earlier case of two PU-occupied channels. This implies that our scheme is scalable with respect to the occupancy of the PU channels. In both

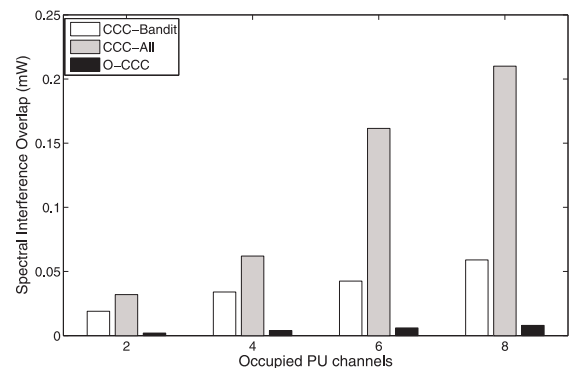


Fig. 7. The spectral interference caused by activating the different number of subcarriers.

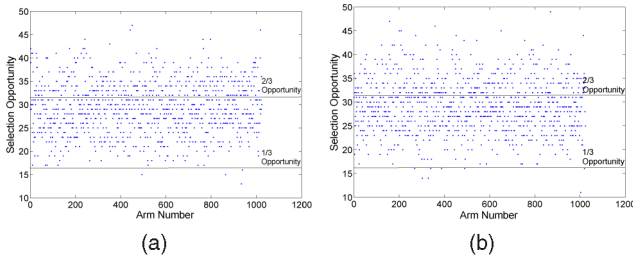


Fig. 8. The number of times an arm is selected (spectrum opportunity) for (a) two and (b) six occupied PU channels is shown, respectively.

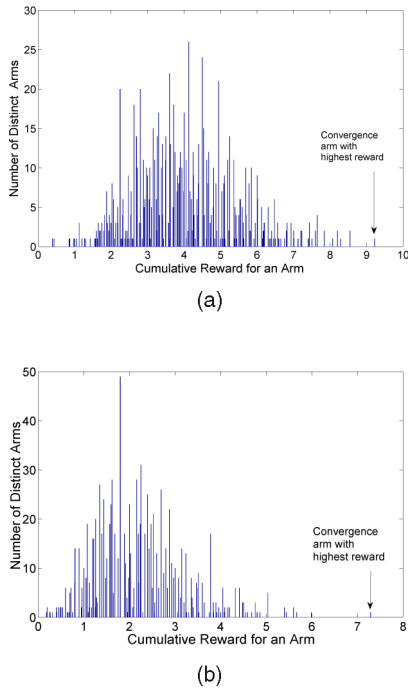


Fig. 9. The number of distinct arms are plotted against the earned reward for (a) two and (b) six occupied PU channels, respectively.

the above cases, the arms are well-explored leading to a progressively decreasing number of arms being preferred for the higher end of the opportunity scale (more than  $\frac{2}{3}$  of the maximum  $\Gamma$ ).

The CR receiver assigns a reward to the sender at the end of each transmission cycle, and the histogram of the cumulative reward is plotted for two and six occupied PU channels in Figs. 9a and 9b, respectively. The x-axis shows the reward collected, and the y-axis gives the number of distinct arms with the same reward value. When the number of affected channels is small, the convergence to the best channel is slow, resulting in higher rewards being accumulated by several different arms (Fig. 9b). However, when the number of affected channels increases, the convergence to the best possible combination is speeded up, and most of the arms incur a reward lower than 2. In each case, there are few arms with the maximum reward earned, proving that our procedure identifies the best arm combination over time and exploits it over the others.

In the discussion this far, we have shown the effect of the arm selection in terms of interference, fairness, and reward.

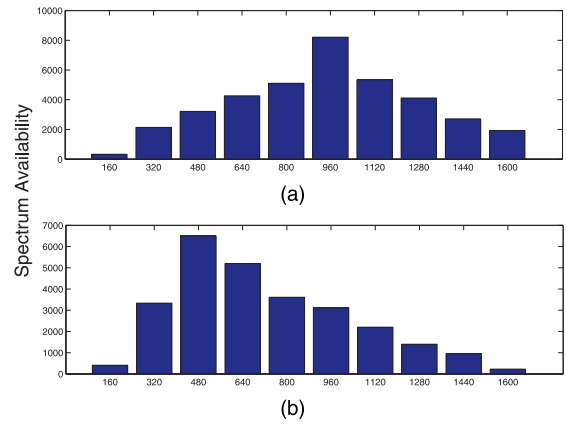


Fig. 10. The number of available transmission opportunities for a given cumulative subcarrier bandwidth are given for (a) two and (b) six occupied PU channels, respectively.

Next, we demonstrate in Fig. 10 1) how much spectrum is available for the CCC (x-axis), and 2) how often it is available (y-axis). For smaller number of occupied channels (2), approximately 960 KHz of usable bandwidth is available for a large part of the network operation, as seen in Fig. 10a. This reduces to about 480 KHz for the case of six occupied PU channels. This spectrum availability takes into account both the initial stage, in which the arms are tried randomly, and also the growing bias toward the most preferred arm seen in the later stage of the operation.

## 6 CONCLUSION

In this work, we proposed an *always-on* CCC design that allows CR users to exchange network information, even under dynamically changing PU activity. Through a feasibility framework, we first identify the static OFDM subcarrier parameters. The choice of the particular guard bands, and hence, the subcarriers that should be active is made independently by the CR users during the network operation. We believe that an efficient CCC is a prerequisite for the higher layer protocols by enabling the sharing of local spectrum information, and facilitates cooperation in the CR network. This area is still in a nascent stage, and further work may proceed along the lines of increasing the data rate for the CCC, and improved learning algorithms that allow a fast convergence on the suitable set of the guard bands.

## ACKNOWLEDGMENTS

This material is based upon work supported by the US National Science Foundation under Grant No. ECCS 0900930.

## APPENDIX

### PROOF OF THEOREM 1

**Proof.** The frequency spectrum of the OFDM subcarriers overlap, allowing a higher number of subcarriers to be accommodated within a given frequency band. Each subcarrier occupies a bandwidth  $B_s$ . Moreover, the separation between the center frequencies of the adjacent

subcarriers, called as subcarrier spacing, is  $\frac{B_s}{2}$ . It can be trivially shown that in a frequency range  $B$ , the actual number of subcarriers, say  $k$ , is given by  $k = 2 \cdot \frac{B}{B_s} - 1$ , where  $B_s > 0$ .

Let  $F_1$  be the ID number of the first central subcarrier  $s_1$  present in the guard band  $G_1$ . The guard bands and the PU channels are as shown in Fig. 1. The frequency range  $B_1$  from the start of the licensed spectrum to the center of  $s_1$  is given by  $B_1 = B_c + \frac{B_g}{2}$ , where the PU channel and the guard interval bandwidths are  $B_c$  and  $B_g$ , respectively. Now, assuming this frequency range  $B$  as a contiguous block, the number of subcarriers, say  $k_1$ , that can be accommodated (and preceding  $s_1$ ) is given by combining the above equations for  $k$  and  $B_1$  as  $k_1 = 2 \cdot \frac{B_c + \frac{B_g}{2}}{B_s} - 1$ .

Now, the ID of  $s_1$  can be written as  $F_1 = k_1 + 1 = \frac{2B_c + B_g}{B_s}$ . Similarly, for the second guard band, the frequency range  $B_2$  before the central subcarrier with ID  $F_2$  is  $B_2 = 2B_c + B_g + \frac{B_g}{2}$ . Along the lines of the calculations for the subcarrier  $s_1$ , we get  $F_2 = 2 \cdot \frac{[2B_c + B_g + \frac{B_g}{2}]}{B_s} = 2 \cdot F_1 + \frac{B_g}{B_s}$ .

Continuing in this way, we observe for the general case,

$$F_i = F_{i-1} + \frac{B_g}{B_s}, \quad i = 2, \dots, N_g \quad (14)$$

From the equation of  $F_i$ , the IDs of central subcarriers can be uniquely identified, proving the statement of Theorem 1.  $\square$

## REFERENCES

- [1] I.F. Akyildiz, W.Y. Lee, and K.R. Chowdhury, "CRAHNs: Cognitive Radio Ad Hoc Networks," *Ad Hoc Networks*, vol. 7, no. 5, pp. 810-836, 2009.
- [2] P. Auer, N. Cesa-Bianchi, Y. Freund, and R.E. Schapire, "The Nonstochastic Multiarmed Bandit Problem," *SIAM J. Computing*, vol. 32, no. 1, pp. 48-77, 2003.
- [3] T. Chen, H. Zhang, G.M. Maggio, and I. Chlamtac, "CogMesh: A Cluster-Based Cognitive Radio Network," *Proc. IEEE Int'l Symp. Dynamic Spectrum Access Networks (DySPAN)*, pp. 168-178, Apr. 2007.
- [4] T. Chen, H. Zhang, M.D. Katz, and Z. Zhou, "Swarm Intelligence Based Dynamic Control Channel in CogMesh," *Proc. IEEE Int'l Conf. Comm. (ICC)*, pp. 123-128, May 2008.
- [5] C. Cordeiro and K. Challapali, "C-MAC: A Cognitive MAC Protocol for Multi-Channel Wireless Networks," *Proc. IEEE Int'l Symp. Dynamic Spectrum Access Networks (DySPAN)*, pp. 147-157, Apr. 2007.
- [6] C. Cormio and K.R. Chowdhury, "A Survey on MAC Protocols for Cognitive Radio Networks," *Ad Hoc Networks*, vol. 7, no. 7, pp. 1315-1329, 2009.
- [7] L.A. DaSilva and I. Guerreiro, "Sequence-Based Rendezvous for Dynamic Spectrum Access," *Proc. IEEE Int'l Symp. Dynamic Spectrum Access Networks (DySPAN)*, pp. 1-7, Oct. 2008.
- [8] R. Fourer, D.M. Gay, and B.W. Kernighan, *AMPL: A Modeling Language for Mathematical Programming*. Duxbury/Brooks/Cole, 2002.
- [9] B. Hamdaoui and K.G. Shin, "OS-MAC: An Efficient MAC Protocol for Spectrum-Agile Wireless Networks" *IEEE Trans. Mobile Computing*, vol. 7, no. 8, pp. 915-930, Aug. 2008.
- [10] J. Jia, Q. Zhang, and X. Shen, "HC-MAC: A Hardware-Constrained Cognitive MAC for Efficient Spectrum Management," *IEEE J. Selected Areas in Comm.*, vol. 26, no. 1, pp. 106-117, Jan. 2008.

- [11] Y.R. Kondareddy and P. Agrawal, "Synchronized MAC Protocol for Multi-Hop Cognitive Radio Networks," *Proc. IEEE Int'l Conf. Comm. (ICC)*, pp. 3198-3202, May 2008.
- [12] L. Le and E. Hossain, "OSA-MAC: A MAC Protocol for Opportunistic Spectrum Access in Cognitive Radio Networks," *Proc. IEEE Wireless Comm. and Networking Conf. (WCNC '08)*, pp. 1426-1430, Mar.-Apr. 2008.
- [13] L. Ma, X. Han, and C.-C. Shen, "Dynamic Open Spectrum Sharing for Wireless Ad Hoc Networks," *Proc. IEEE Int'l Symp. Dynamic Spectrum Access Networks (DySPAN)*, pp. 203-213, Nov. 2005.
- [14] L. Ma, C.-C. Shen, and B. Ryu, "Single-Radio Adaptive Channel Algorithm for Spectrum Agile Wireless Ad Hoc Networks," *Proc. IEEE Int'l Symp. Dynamic Spectrum Access Networks (DySPAN)*, pp. 547-558, Apr. 2007.
- [15] P. Pawelczak, R.V. Prasad, L. Xia, and I.G. Niemegeers, "Cognitive Radio Emergency Networks—Requirements and Design," *Proc. IEEE Int'l Symp. Dynamic Spectrum Access Networks (DySPAN)*, pp. 601-606, Nov. 2005.
- [16] R. Rajbanshi, A.M. Wyglinski, and G.J. Minden, "Peak-to-Average Power Ratio Analysis for NC-OFDM Transmissions," *Proc. IEEE Vehicular Technology Conf. (VTC)*, pp. 1351-1355, Sept.-Oct. 2007.
- [17] H. Su and X. Zhang, "Opportunistic MAC Protocols for Cognitive Radio Based Wireless Networks," *Proc. Ann. Conf. Information Sciences and Systems*, pp. 363-368, Mar. 2007.
- [18] H. Su and X. Zhang, "CREAM-MAC: An Efficient Cognitive Radio-Enabled Multi-Channel MAC Protocol for Wireless Networks," *Proc. IEEE Int'l Symp. World of Wireless, Mobile and Multimedia Networks*, pp. 1-8, June 2008.
- [19] P. Santi, "The Critical Transmitting Range for Connectivity in Mobile Ad Hoc Networks," *IEEE Trans. Mobile Computing*, vol. 4, no. 3, pp. 310-317, May/June 2005.
- [20] J. Zhao, H. Zheng, and G.-H. Yang, "Spectrum Agile Radios: Utilization and Sensing Architecture," *Proc. IEEE Int'l Symp. Dynamic Spectrum Access Networks (DySPAN)*, pp. 259-268, Nov. 2005.



**Kaushik R. Chowdhury** received the BE degree in electronics engineering with distinction from VJTI, Mumbai University, India, in 2003, the MS degree in computer science from the University of Cincinnati, Ohio, in 2006, and the PhD degree from the Georgia Institute of Technology, Atlanta, in 2009. His MS thesis was given the Outstanding Thesis Award jointly by the Electrical and Computer Engineering and Computer Science Departments at the University of Cincinnati. He has also won the BWN Researcher of the Year Award during his PhD studies in 2007, and the Best Paper Award in the Ad Hoc and Sensor Networks Symposium at the IEEE ICC Conference in 2009. He is an assistant professor in the Electrical and Computer Engineering Department at Northeastern University, Boston, Massachusetts. His expertise and research interests lie in wireless cognitive radio ad hoc networks, energy harvesting, and multimedia communication over sensors networks. He is a member of the IEEE.



**Ian F. Akyildiz** received the BS, MS, and PhD degrees in computer engineering from the University of Erlangen-Nuremberg, Germany, in 1978, 1981, and 1984, respectively. Currently, he is the Ken Byers distinguished chair professor with the School of Electrical and Computer Engineering, Georgia Institute of Technology, Atlanta, the director of Broadband Wireless Networking Laboratory, and chair of the Telecommunication Group at the Georgia Institute of Technology. In June 2008, he became an honorary professor with the School of Electrical Engineering at the Universitat Politècnica de Catalunya (UPC) in Barcelona, Spain. He is also the director of the newly founded N3Cat (NaNoNetworking Center in Catalunya). He is the editor-in-chief of *Computer Networks* (Elsevier) and the founding editor-in-chief of *Ad Hoc Networks* (Elsevier), *Nano Communications Networks* (Elsevier), and *Physical Communication* (Elsevier). He serves on the advisory boards of several research centers, journals, conferences, and publication companies. He became an IEEE fellow in 1996 and an ACM fellow in 1997. He has received numerous awards from the IEEE and the ACM. His research interests are in nanonetworks, cognitive radio networks, and wireless sensor networks.